Statistical Spatial Filtering for a P300-based BCI: Tests in able-bodied, and Patients with Cerebral Palsy and Amyotrophic Lateral Sclerosis

Gabriel Pires[a,*], Urbano Nunes[a], Miguel Castelo-Branco[b]

[a] *Institute for Systems and Robotics (ISR), University of Coimbra, 3030-290 Coimbra, Portugal*
[b] *Biomedical Institute for Research in Light and Image (IBILI), University of Coimbra, 3000-548 Coimbra, Portugal*

Abstract

The effective use of brain-computer interfaces (BCI) in real-world environments depends on a satisfactory throughput. In a P300-based BCI, this can be attained by reducing the number of trials needed to detect the P300 signal. However, this task is hampered by the very low signal-to-noise-ratio (SNR) of P300 event related potentials. This paper proposes an efficient methodology that achieves high classification accuracy and high transfer rates for both disabled and able-bodied subjects in a standard P300-based speller system. The system was tested by three subjects with cerebral palsy (CP), two subjects with amyotrophic lateral sclerosis (ALS), and nineteen able-bodied subjects.

The paper proposes the application of three statistical spatial filters. The first is a beamformer that maximizes the ratio of signal power and noise power (Max-SNR). The second is a beamformer based on the Fisher criterion (FC). The third approach cascades the FC beamformer with the Max-SNR beamformer satisfying simultaneously sub-optimally both criteria (C-FMS). The calibration process of the BCI system takes about 5 minutes to collect data and a couple of minutes to obtain spatial filters and classification models.

Online results showed that subjects with disabilities have achieved, on average, an accuracy and transfer rate only slightly lower than able-bodied subjects. Taking 23 of the 24 participants, the averaged results achieved

---

*Corresponding author. Phone: +351962782654
Email address: gpires@isr.uc.pt (Gabriel Pires)

a transfer rate of 4.33 symbols per minute with a 91.80% accuracy, corresponding to a bandwidth of 19.18 bits per minute. This study shows the feasibility of the proposed methodology and that effective communication rates are achievable.

Keywords: Brain computer interface, electroencephalography, P300, spatial filtering, signal-to-noise ratio.

1. Introduction

Brain computer interfaces (BCI) based on electroencephalography (EEG) emerge as a feasible type of human-computer and human-machine interfaces that open new communication channels to persons suffering from severe motor disabilities, such as amyotrophic lateral sclerosis (ALS), full paraplegia and certain types of cerebral palsy, without recurring to the conventional motor output pathways. For some of these patients, standard interfaces such as speech recognition, eye tracking and head or teeth switches are not suitable because they suffer from total lack of motor control or very low dexterity affecting head, limbs, eyes and speech.

Scalp recorded EEG is a non-invasive technique that presents a very good temporal resolution and requires relatively low-cost devices. These are the two main reasons that explain its widespread use in BCI. However, EEG presents a poor spatial resolution mainly due to volume conduction (Srinivasan et al., 1998). This phenomena associated with the presence of artifacts such as muscular activity, external stimuli, environmental noise and spontaneous ongoing EEG, substantially degrade the signal-to-noise ratio (SNR), particularly in event related potentials (ERP). Moreover, EEG signals are nonstationary and present inter-subject and within-subject variability. The decoding of user intentions from brain patterns therefore requires the application of signal processing and pattern recognition techniques that can enhance the desired components and attenuate noise from EEG data. In the context of classification, another important issue is the reduction of feature dimensionality to attenuate overfitting of training data and to increase the computational efficiency of algorithms for real time operation (Hall, 2000).

Several approaches have been proposed for classification in P300-based BCI systems. One common practice is to apply feature extraction, or simply decimation, on each raw channel, and then concatenate the features from every channel into a feature vector used for classification (Thulasidas et al., 2006; Lenhardt et al., 2008). This approach can be combined with feature selection algorithms, via wrapper or filter methods, able to find the most discriminative features (Rakotomamonjy and Guigue, 2008; Hoffmann et al., 2008b). One popular combination of classification and feature selection is the stepwise linear discriminant analysis (SWLDA), which has demonstrated good classification results (Farwell and Donchin, 1988; Donchin et al., 2000; Krusienski et al., 2008; Townsend et al., 2010). Other efficient classification methods were already proposed such as support vector machine (SVM) (Rakotomamonjy and Guigue, 2008; Kaper et al., 2004) and Fisher linear discriminant analysis (FLDA) (Hoffmann et al., 2008a). See (Krusienski et al., 2006) for a comparison of several P300 classification methods. Feature selection is a way of increasing the SNR because it removes noisy and non-discriminative features, but it does not take full advantage of the spatial combination of multichannel data as it happens in spatial filtering. When signal and noise have different spatial foci, spatial filtering can decompose raw signals into different components separating noise and meaningful components, leading to an enhanced SNR. Feature selection algorithms can still be applied after spatial filtering further improving the SNR. Spatial filtering assumes particular importance when the temporal frequency spectrum of noise and interferences overlaps the temporal frequency spectrum of the transient P300 signal, since temporal filtering is not able to separate noise from signal (see section 3.1).

Three spatial filtering methods are commonly applied in BCI: independent component analysis (ICA), principal component analysis (PCA) and common spatial patterns (CSP). Both ICA and PCA are mainly used on an unsupervised way, the former for separation of multichannel EEG data into statistically independent components, and the second for dimensionality reduction (Lenhardt et al., 2008) and denoising. Most of the ICA applications have been on offline neurophysiologic analysis (Makeig et al., 1999), and for strong artifact removal, such as eye blinking, eye movement and muscular activity (Jung et al., 2000; Müller et al., 2004). Still, there are successful online and offline applications of ICA in the context of P300-based systems, as you can see respectively in (Serby et al., 2005; Piccione et al., 2006) and (Xu et al., 2004). The CSP method is a supervised technique that relies on the simultaneous diagonalization of two covariance matrices, maximizing the differences between two classes (Fukunaga and Koontz, 1970). It was first applied in (Soong and Koles, 1995) for localization of neurophysiologic features and since then it has been mainly applied in motor imagery based BCIs (Müller-Gerking et al., 1999; Ramoser et al., 2000; Blanchard and Blankertz, 2004; Li et al., 2004; Lemm et al., 2005; Dornhege et al., 2006), outperforming ICA and classical EEG re-referencing montages such as Laplacian derivations (Naeem et al., 2006). As concerns the effective use of CSP for P300 detection, see (Krusienski et al., 2007) for a variant of CSP called common spatio-temporal patterns (CSTP) and (Pires et al., 2009) where a straightforward application of CSP was proposed. In (Rivet et al., 2009) it is proposed the xDAWN algorithm, which estimates spatial filters that find the evoked subspace by maximizing the signal-to-signal plus noise ratio. In other contexts than BCI, many other spatial filtering techniques have been proposed specifically for ERP denoising (de Cheveigne and Simon, 2008; Ivannikov et al., 2009).

This paper analyzes and assesses the application of several statistical beamformers in a P300 based BCI, with experimental testing on a standard row-column speller paradigm. Beamforming techniques were originally developed in the field of antenna and sonar array signal processing (Van Veen and Buckley, 1988; Trees, 2002) and are currently used in many other areas including magnetoencephalography (MEG) and EEG source reconstruction/localization (Van Veen et al., 1997; Sekihara et al., 2001; Grosse-Wentrup et al., 2009).

Firstly, we propose a beamformer based on the classical SNR maximization criterion (Max-SNR) (Van Veen and Buckley, 1988). The filter is obtained from the eigenvector that maximizes the output ratio of signal and noise powers. The method works blindly, i.e., it does not use geometrical information about the sensor array or the underlying sources. It requires the estimation of covariances matrices associated with periods of the P300 signal, and periods of only noise-plus-interference. Secondly, a beamformer based on the Fisher Criterion (FC) is proposed following the same eigenvector-based principle used in Max-SNR. The method extends the well known Fisher linear discriminant (FLD) to the spatial domain using an approach similar to (Hoffmann et al., 2006). Third, the two beamformers are cascaded in order to satisfy simultaneously in a suboptimum way both criteria (Fukunaga, 1990, Ch.10). This spatial filter is henceforth designated C-FMS.

Experimental assessment of the spatial filters show the effective improvement as concerns SNR and classification accuracy. Their performance is compared with the one obtained with best channel and with Laplacian spatial filtering. The Laplacian method is a high-pass spatial filter that computes for each electrode the instantaneous second derivative of the spatial voltage

Figure 1: Screenshot of 6×6 matrix speller paradigm.

distribution, emphasizing localized activity and attenuating surrounding activity. It is an unsupervised technique that significantly increases the SNR and thereby increases the classification accuracy (McFarland et al., 1997). Two classification methodologies, one combining the average of the signal epochs and the other combining the *a posteriori* probabilities, are compared. The system requires a short calibration time of about 7 minutes, more exactly, 5 minutes to collect data plus 2 minutes to obtain spatial filters and classification models. The C-FMS filter combined with feature selection and a Bayesian classifier is tested online on a group of 19 able-bodied participants and 5 disabled participants. For performance comparison purposes, the C-FMS method is also tested on the data sets of the BCI-competition 2003 (BCI-Competition, 2003).

Although the methods are applied in a P300-based BCI framework, they can also be used to reduce the recording duration in patient examinations, when P300 detection is used as a diagnostic tool (e.g., cognitive impairments, neurological and psychiatric disorders) (Mell et al., 2008).

2. Paradigm, Data Acquisition and Participants

2.1. Participants

The experiments were performed by nineteen able-bodied volunteers, three subjects with cerebral palsy (CP), and two subjects with amyotrophic lateral sclerosis (ALS). All participants gave informed consent to participate in the study. Fourteen of the able-bodied subjects and the five disabled

Table 1: Clinical data of CP and ALS patients

Patient	Age	Sex	Diagnosis	Time since diagnosis (years)
S20	18	F	CP: spastic tetraparesis and dysarthria	posnatal
S21	34	M	CP: spastic tetraparesis and dysarthria, and involuntary movements with high amplitude	perinatal
S22	46	M	CP: spastic tetraparesis, dysarthria and discal hernia C3-C4	perinatal
S23	67	F	bulbar ALS (FRS-r 46)	7
S24	75	F	bulbar ALS (FRS-r 40)	1

subjects never had used a BCI before. Table 1 presents a summary of clinical data of disabled subjects. The three subjects with CP present severe spastic tetraparesis (neuromuscular mobility impairment characterized by hypertonic muscle tone affecting all four limbs and trunk) and dysarthria (speech disorder characterized by poor articulation), and are all confined to a wheelchair. Subject S20 steers the wheelchair using an head-switch that selects the direction via a scanning interface, subject S21 uses an adapted joystick controlled by the right foot, and subject S22 controls the wheelchair with the chin. All present involuntary movements which are more pronounced on subject S21. Subjects S23 and S24 present a bulbar-onset ALS whose main signs are dysarthria and dysphagia (swallowing difficulty). Subject S23 also begins to exhibit muscular weakness in upper limbs with distal predominance. The degree of disability was rated by using the revised ALS functional rating scale (ALSFRS-r) where 48 is normal and 0 a complete loss of functionality (Cedarbaum et al., 1999). Spoken communication with subjects S20-S23 was hard, and impossible with subject S24. All patients presented normal cognitive capabilities. The group of able-bodied volunteers was composed of 10 males and 9 females with ages from 18 to 42 years old, averaging 30.1 years old.

2.2. Paradigm and procedure

The speller system is based on the paradigm proposed by Farwell and Donchin (Farwell and Donchin, 1988) as shown in Fig.1. The speller paradigm presents a 6×6 matrix with the alphabet letters and other useful symbols such as the 'spc' and 'del'. The rows and columns are intensified during 100 ms with an inter-stimulus interval (ISI) settled to 200 ms. For every complete scanning (round), each row and column is intensified once in a random order. The target events are the row and column that include the symbol mentally selected by the user. All other rows and columns are the non-target events. Thus, for each round there are 2 target events and 10 non-target events, which corresponds to a target event probability of 2/12. It is expected that target events will elicit a P300 ERP. The EEG signals are recorded and synchronously marked with event codes. The data segment associated to each event is called an epoch and has a duration of 1 second. The interval between each group of rounds is called inter-trial interval (ITI). This interval was settled to 2.5 seconds to allow the user to switch the attention focus for a new letter mentally selected.

The experiments took place on regular rooms in an environment with some noise and people moving around. The sessions with CP and ALS subjects took place respectively at the facilities of the Cerebral Palsy Association of Coimbra (APCC) and the Hospitals of the University of Coimbra (HUC). The sessions with able-bodied participants took place at working labs. The experiments consisted of a calibration phase and of an online phase. Before the calibration phase, the subjects were instructed to be relaxed and attend the desired target, mentally counting the number of intensifications of target rows and columns. The able-bodied and ALS subjects were seated on a standard chair, while the CP subjects were seated at their own wheelchairs. A 15" computer screen was positioned in front of the participants at about 60-70 cm. It was asked only to the able-bodied subjects to avoid blinking and moving the eyes.

During the calibration phase, the subjects attended the letters of the word 'INTERFACE' (9 characters) which were successively provided at the top of the monitor (Fig. 1). Each row and column was repeated 10 times for each letter. Therefore, the data collected during the calibration phase consisted of 180 target epochs and 900 non-target epochs. This calibration session took about 5 minutes, and after that, the classification models were trained from collected and labeled data, taking only a couple of minutes. The online sessions took place just after the calibration phase.

The EEG activity was acquired with a g.tec gUSBamp amplifier. Signals were recorded from 12 Ag/Cl electrodes at positions Fz, Cz, C3, C4, CPz, Pz, P3, P4, PO7, PO8, POz and Oz of the internacional extended 10-20 standard system with a g.tec cap. The electrodes were referenced to the right ear lobe and the ground was placed at AFz. Signals were sampled at

256 Hz, and filtered by a 0.1-30 Hz bandpass filter and a 50 Hz notch filter. The electrodes impedance varied from subject to subject, but were almost always kept under $10K\Omega$.

3. Signal Processing and Classification Methods

3.1. Assumptions and notation

Consider an EEG epoch $\mathbf{X}$ defined as a time sequence of measures, $\mathbf{X} = [\mathbf{x}(t_1) \quad \mathbf{x}(t_2) \quad \cdots \quad \mathbf{x}(t_T)]$, where T is the number of time samples and $\mathbf{x}(t)$ is a column vector with dimension N (number of EEG channels). Therefore, each epoch is represented by a spatio-temporal matrix $\mathbf{X}$ with dimension $N \times T$ (in our case, $N = 12$ channels and $T = 256$ samples). Target and non-target epochs are represented respectively by $\mathbf{X}_+$ and $\mathbf{X}_-$, where the subscripts $_+$ and $_-$ stand respectively for target and non-target.

Let us consider target epochs modeled according to

$$\mathbf{X}_{+,k} = \mathbf{S}_k + \mathbf{V}_k \tag{1}$$

where $\mathbf{X}_{+,k}$ is the k_{th} recorded epoch and $\mathbf{S}_k$ is the k_{th} P300 signal, measured in the N dimensional space. $\mathbf{V}_k$ contains activity from ongoing EEG, plus the interference from not-attended flashes, plus white noise. Non-target epochs occur immediately before target epochs and thus the activity should be similar to $\mathbf{V}_k$. Hence, $X_{-,k}$ is modeled as the noise and interference part of the measured target epochs

$$\mathbf{X}_{-,k} = \mathbf{V}_k. \tag{2}$$

Models (1) and (2) were experimentally sustained by means of a frequency analysis. It consisted of calculating and analyzing the FFT spectra over representative data collected from one session (180 target epochs and 900 non-target epochs). Color maps in Fig. 2(a) and Fig. 2(b) represent respectively the FFT spectra of 90 target and 90 non-target epochs measured at channel Pz. The spectra for both conditions, $\mathbf{X}_+$ and $\mathbf{X}_-$, present similar frequency distributions. This overlapping of spectra is evidenced in the example of a single realization in Fig. 2(c). This shows, firstly, that much of the non-target activity is contained in target epochs, and secondly, that temporal filtering is insufficient to remove noise from target epochs, and thus it should be used carefully. Figure 2(d) presents the average of the FFT spectra of target and non-target epochs. The average attenuates the

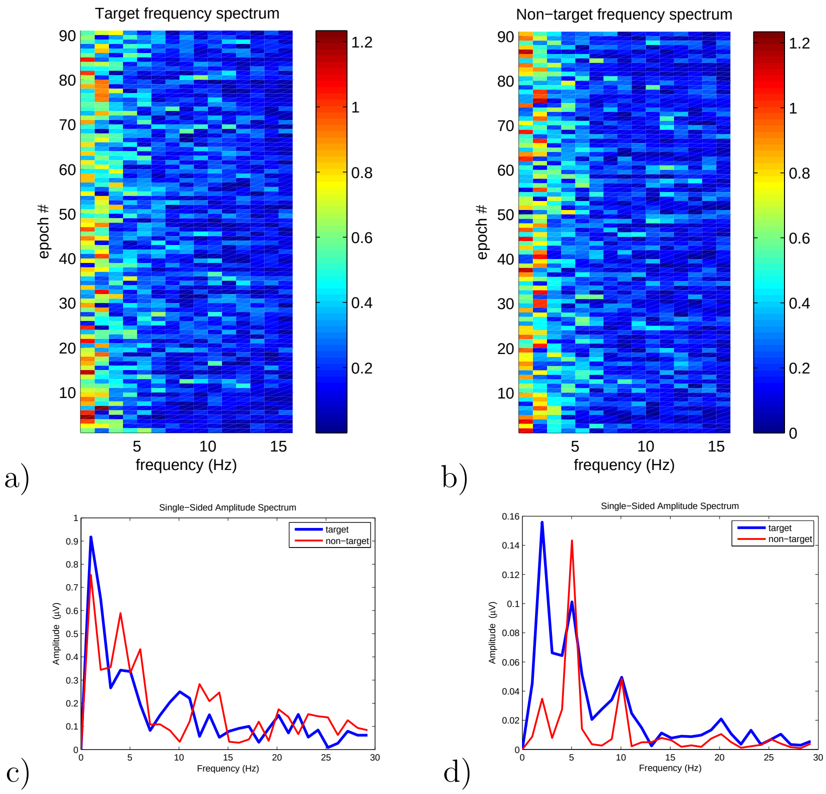

Figure 2: FFT spectrum of a representative data set of one session (180 target and 900 non-target epochs) measured at channel Pz; (a) Color map of the FFT spectra over 90 out of the 180 target epochs; (b) Color map of the FFT spectra over 90 out of the 900 non-target epochs; (c) Example of one FFT of a single epoch (target and non-target); (d) Average of the FFT spectra of all epochs (180 FFTs of target epochs and 900 FFTs of non-target epochs).

spectrum of random components, and emphasizes the spectrum of the P300 ERP and other uncorrelated interfering signals. A strong interference at 5 Hz appears in the target spectrum (see Fig. 2(d)). This interference comes from the rows/columns flashing with an ISI of 200 ms, i.e, 5 Hz (see its effect in time domain in Fig. 3). These stimuli generate a steady state visual evoked potential (SSVEP) at 5 Hz, and a 2nd harmonic at 10 Hz as well. This 2nd harmonic affects target epochs with less impact because it does not overlap the spectrum of the P300 signal.

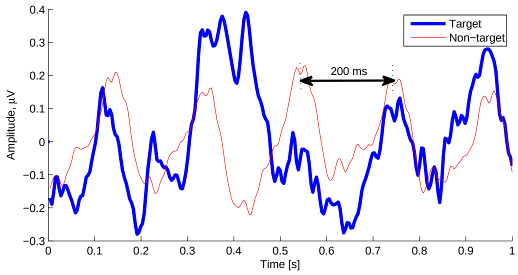

Figure 3: Average of 180 unfiltered target epochs and 900 unfiltered non-target epochs recorded at channel Pz. The result evidences an oscillatory component with 200 ms period in non-target epochs, which is also visible in target epochs.

3.2. Spatial Filtering

A spatial filter is generically an weighting vector, w, that combines the data of N channels at each time instant t

$$\mathrm{y}_j(t) = \sum_{i=1}^{N} \mathrm{w}_{ij}\mathrm{x}_i(t) \quad , j = 1, \cdots, N \tag{3}$$

where y_j is the output projection obtained from input channels x_i, which can be denoted in the matrix notation from:

$$\mathbf{Y} = W'\mathbf{X} \tag{4}$$

where $'$ denotes the transpose operator.

3.2.1. Max-SNR beamformer

In this first approach, the spatial filtering of P300 is stated as a denoising problem. The solution is an optimum beamformer, based on statistical data, that maximizes the output SNR

$$\mathrm{SNR} = \frac{\mathrm{E}[W'\mathbf{S}\mathbf{S}'W]}{\mathrm{E}[W'\mathbf{X}_{-}\mathbf{X}'_{-}W]} \backsimeq \frac{W'\overline{\mathbf{R}}_{+}W}{W'\overline{\mathbf{R}}_{-}W} \tag{5}$$

where W is the weighting vector, $\mathrm{E}[\cdot]$ represents the expectation operator, and the matrices $\overline{\mathbf{R}}_{+}$ and $\overline{\mathbf{R}}_{-}$ are the estimated covariance matrices for target and non-target. The maximum SNR is obtained by maximizing the discriminative Rayleigh quotient in (5). The optimal W is the eigenvector associated to the largest eigenvalue. The solution is achieved by finding the generalized eigenvalue decomposition that satisfies the equation

$$\overline{\mathbf{R}}_+ W = \overline{\mathbf{R}}_- W \Lambda \tag{6}$$

where Λ is the eigenvalue matrix. The eigenvectors W are obtained from the eigenvalue decomposition of $(\overline{\mathbf{R}}_-)^{-1}\overline{\mathbf{R}}_+$ provided that $\overline{\mathbf{R}}_-$ is nonsingular. The principal eigenvector $W^{(1)}$ maximizes the SNR, and therefore the output of the beamformer is given by

$$\mathbf{y} = W^{(1)\prime}\mathbf{X}. \tag{7}$$

The $N \times T-$dimensional measurement $\mathbf{X}$ is transformed into a 1-dimensional subspace, $1 \times T$. This reduction of the feature space is an important achievement for subsequent classification.

The matrices $\overline{\mathbf{R}}_+$ and $\overline{\mathbf{R}}_-$ are estimated from the average over the epochs within each class, gathered during calibration sessions. Consider the $N \times N$ normalized spatial covariance for each epoch k given by $\mathbf{R}_k = \mathbf{X}_k\mathbf{X}_k'/tr(\mathbf{X}_k\mathbf{X}_k')$, then, $\overline{\mathbf{R}}_+$ and $\overline{\mathbf{R}}_-$ are computed from

$$\overline{\mathbf{R}}_+ = \frac{1}{K_+}\sum_{k=1}^{K_+}\mathbf{R}_{+,k} \quad \text{and} \quad \overline{\mathbf{R}}_- = \frac{1}{K_-}\sum_{k=1}^{K_-}\mathbf{R}_{-,k} \tag{8}$$

where K_+ and K_- are the number of target and non-target training samples. The size of the target and non-target classes is highly unbalanced and therefore a regularization of the covariance matrices according to

$$\overline{\mathbf{R}}_+ W = (\overline{\mathbf{R}}_+ + \alpha\overline{\mathbf{R}}_-)W\Lambda, \tag{9}$$

where $\alpha \leq 1$, can alleviate overfitting and improve class discrimination.

The Max-SNR solution (6) is similar to that obtained from CSP, which can also be stated as a generalized eigenvalue problem as can be seen in (Tomioka et al., 2007). The Max-SNR can be regarded as a particular case of CSP.

3.2.2. FC Beamformer

The Max-SNR criterion relies on the ratio of signal and noise cross-powers. From a pattern recognition perspective, other criteria can be investigated to implement a beamformer. One of such criteria is the Fisher's criterion (FC)

(Duda et al., 2001), which aims to increase the separation between classes while minimizing the variance within a class (Fisher linear discriminant - FLD). This concept can easily be extrapolated to the spatial domain using spatio-temporal data as was done in Max-SNR (section 3.2.1). The FC takes into consideration the difference between target and non-target spatio-temporal patterns. Then it is expected that the spatial filter maximizes the spatio-temporal differences, leading to an enhancement of specific subcomponents of the ERP. The FC is given by the Rayleigh quotient

$$J(W) = \frac{W'\mathbf{S}_b W}{W'\mathbf{S}_w W} \tag{10}$$

where $\mathbf{S}_b$ is the spatial between-class matrix and $\mathbf{S}_w$ is the spatial within-class matrix. The optimum filter W is found solving the generalized eigenvalue problem

$$\mathbf{S}_b W = \mathbf{S}_w W \Lambda. \tag{11}$$

The selected filter is the eigenvector associated with the largest eigenvalue, i.e., $W^{(1)}$, and the spatial filter output is obtained by applying expression (7).

Taking the spatio-temporal matrix $\mathbf{X}_k$ (dimension $N \times T$) from each epoch k, the matrices $\mathbf{S}_b$ and $\mathbf{S}_w$ are computed from

$$\mathbf{S}_b = \sum_i p_i(\overline{\mathbf{X}}_i - \overline{\mathbf{X}})(\overline{\mathbf{X}}_i - \overline{\mathbf{X}})' \tag{12}$$

and

$$\mathbf{S}_w = \sum_i \sum_{k \in C_i} (\mathbf{X}_{i,k} - \overline{\mathbf{X}}_i)(\mathbf{X}_{i,k} - \overline{\mathbf{X}}_i)' \tag{13}$$

where $i \in \{+, -\}$ and, C_+ and C_- represent respectively the target and non-target classes, and p_i is the class probability. The average of the epochs in class C_i and the average of all epochs are respectively denoted $\overline{\mathbf{X}}_i$ and $\overline{\mathbf{X}}$, with

$$\overline{\mathbf{X}}_i = \frac{1}{K_i} \sum_{k=1}^{K_i} \mathbf{X}_{i,k} \quad \text{and} \quad \overline{\mathbf{X}} = \frac{1}{K} \sum_{k=1}^{K} \mathbf{X}_k \tag{14}$$

where K_i is the number of epochs in class C_i and K is the total number of epochs. To increase generalization, $\mathbf{S}_w$ in (11) can be regularized according to

$$\mathbf{S}_b W = [(I - \theta)\mathbf{S}_w + \theta I] W \Lambda \tag{15}$$

where θ is the regularized parameter that can be adjusted from training data to increase class discrimination.

3.2.3. C-FMS beamformer

In order to satisfy both Max-SNR and FC, a cascade of the two spatial filters is proposed using a suboptimum approach (Fukunaga, 1990, Ch.10). FC is applied first since it is more discriminative than Max-SNR. The first transform is obtained from

$$\mathbf{Y} = W_1{}'\mathbf{X} \tag{16}$$

where W_1 is the spatial filter computed according to (15). The first feature vector is obtained from the first projection

$$\mathbf{y_1} = W_1^{(1)\prime}\mathbf{X}. \tag{17}$$

The feature vector $\mathbf{y_1}$ preserves the information about FC while the remaining components in the $(N-1)-$dimensional space are used for a second transform

$$\mathbf{Z} = W_2{}'\mathbf{Y}^{(2:N)} \tag{18}$$

where the spatial filter W_2 is estimated according to (9) taking $\mathbf{Y}^{(2:N)}$ data from the 1st stage of cascade (16). The first projection satisfies the Max-SNR criterion

$$\mathbf{z_1} = W_2^{(1)\prime}\mathbf{Z}. \tag{19}$$

The concatenation of the two projections

$$\mathbf{v} = [\mathbf{y_1} \quad \mathbf{z_1}] \tag{20}$$

maximizes both FC and max-SNR criteria in a suboptimum way.

3.3. Classification and Feature Selection

In terms of pattern recognition, the oddball paradigm reduces a *n-events* detection to a binary discrimination problem, i.e., the discrimination between target events (desired row and column events: *two* of the *n-events*) and non-target events (remaining *(n - 2) events*). The final decision to detect the target is reached combining the n binary classification outputs.

The classification is performed by a Bayesian classifier. It presents properties that makes it a suitable option for our classification problem. Namely, it offers an easy way to include prior probabilities and to control false positive and false negative rates, it returns probability values that can be used for combination of event classification outputs, and the parameters are easily tuned requiring a short period of training. Furthermore, its application is straightforward and computationally undemanding. More powerful classification algorithms could be implemented such as SVM or neural networks, further improving the classification results presented in this study. The comparison of classification methods is however beyond the scope of this paper. After spatial filtering, the feature space is an unidimensional vector $\mathbf{y} = [y(t_1) \quad y(t_2) \quad \cdots \quad y(t_T)]$. The features are scored according to the r-square discrimination (square of the Pearson's correlation coefficient) between target and non-target epochs, and then the features with higher score are selected for classification. The Bayesian classifier is presented in its naïve form (NB), i.e., it assumes that the features are conditionally independent. Under this assumption, the joint pdf is given by the product of the pdf of each individual feature

$$\begin{aligned} p(\mathbf{y}|C_i) &= \prod_{j=1}^{N_f} p(\mathbf{y}(j)|C_i) = \\ &= \prod_{j=1}^{N_f} \frac{1}{\sqrt{2\pi}\sigma_i(j)} \exp\left(-\frac{(y(j)-\mu_i(j))^2}{2\sigma_i^2(j)}\right) \end{aligned} \tag{21}$$

where each feature j is assumed to have a normal distribution $\mathcal{N}(\mu_i(j), \sigma_i^2(j))$. The number of features is defined by N_f, and C_i ($i \in \{+,-\}$) represents the target and non-target classes. The *a posteriori* probability $p(C_i|\mathbf{y})$ is computed from the conditional probabilities using the Bayes theorem:

$$P(C_i|\mathbf{y}) = \frac{P(C_i)p(y|C_i)}{p(\mathbf{y})}. \tag{22}$$

The prior probabilities $P(C_i)$ are respectively $2/12$ and $10/12$ for target and non-target. The class is detected using the following maximum *a posteriori* decision rule

$$\hat{c} = \arg\max\{P(C_+|\mathbf{y}), P(C_-|\mathbf{y})\}. \tag{23}$$

4. Results

The proposed spatial filter methods were experimentally evaluated through two assessment parameters: SNR measure and classification accuracy.

The data sets for this analysis were obtained for each participant during the calibration phase, according to the protocol defined in section 2. The beamformers Max-SNR, FC and C-FMS were estimated from calibration data sets using respectively (9), (15), and combining (15) with (9) following the methodology in section 3.2.3. The parameters α in (9) and θ in (15) were pre-set with the same values for all participants.

4.1. SNR and Discrimination Enhancement

One natural measure to evaluate the performance of the spatial filters is the SNR. It was estimated according to (Lemm et al., 2006)

$$\begin{aligned}\mathrm{SNR}(\mathbf{y}) &= 10\log\frac{\mathrm{Var}_t(\mathrm{E}_k[\mathbf{y}])}{\mathrm{E}_k[\mathrm{Var}_t(\mathbf{y}-\mathrm{E}_k[\mathbf{y}])]}\\ &= 10\log\frac{\mathrm{Var}_t(\bar{\mathbf{y}})}{\mathrm{E}_k[\mathrm{Var}_t(\mathbf{y}-\bar{\mathbf{y}})]}\end{aligned} \tag{24}$$

where Var_t is the temporal variance of the ERP signal and $\mathrm{E}_k[\cdot]$ denotes the mathematical expectation operator, applied over all K epochs of calibration data sets. To assess the improvement performance, the SNRs of Max-SNR and FC beamformers were respectively compared with: 1) the SNR of the best channel; 2) the averaged SNR over the 12 channels; and 3) the SNR of Laplacian derivations at channels Cz and Pz, taking respectively (Fz, C3, C4, Pz) and (Cz, Oz, PO7, PO8) as surrounding electrodes. The SNR of C-FMS was not computed because its first projection coincides with the FC beamformer, and thereby would lead to the same results. The SNR estimates were then averaged taking 23 of the 24 subjects, achieving the results in Fig. 4. The results were obtained for different number of averaged epochs[1], K, ($K = 1\cdots 7$), thus simulating a different number of repetitions of the events. The data sets from subject S21 were discarded in the analysis because this subject did not evoke a visible P300. The results are statistically evaluated with a t-test. For single epochs ($K = 1$), the SNR is -6.36 dB for FC beamformer, which is significantly higher than the values obtained respectively for: 1) all-channel average, -14.60 dB, ($t(22) = 9.93$, $p \leq 0.001$);

[1]It is important to note that, when averaging, the number of samples of the data sets is reduced by the number of epochs, K, used in the average. For instance, if $K = 2$ the number of target and non-targets epochs will be respectively $180/2 = 90$ and $900/2 = 450$; for $K = 3$, $180/3 = 60$ and $900/3 = 300$, and so on.

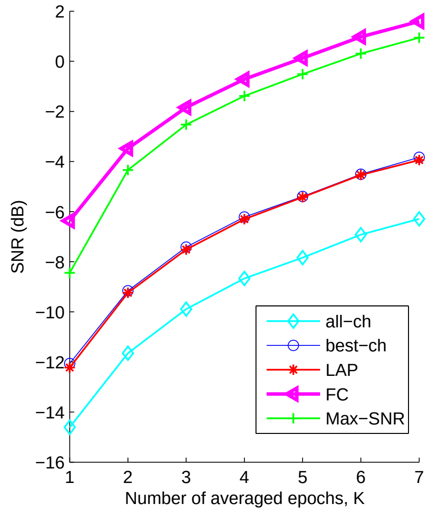

Figure 4: SNR estimated from 23 subjects. Analysis for a single epoch (K=1) and K-epoch average $K = 2 \cdots 7$.

2) best-channel, -12.05 dB ($t(22) = 10.68$, $p \leq 0.001$); 3) Laplace derivations, -12.22 dB ($t(22) = 9.05$, $p \leq 0.001$); and 4) Max-SNR, -8.44 dB ($t(22) = 6.68$, $p \leq 0.001$). In the case of K-epoch average, $K = 2 \cdots 7$, the spatial filters were applied to the average of K epochs and then the SNR was computed from the spatial projection. The positive SNR margin between FC and, all-channel average, best channel, Laplace derivations and Max-SNR, are respectively 8.18 dB, 5.68 dB, 5.76 dB and 0.87 dB. These differences are approximately constant over the $K = 2 \cdots 7$ averaged epochs, and always statistically significant ($p \leq 0.001$). For all methods, as the number of epochs taken for average increases, the SNR also increases, which was expected given the phase-locked properties of ERPs. The SNR improvements led to an enhancement of the ERP and thereby to an increased discrimination between target vs. non-target. The statistical r-square measure was used to assess this discrimination. The color maps in Fig. 5 compares the r-square values before spatial filtering (top) and after C-FMS spatial filtering (bottom), for a representative data set with 180 target epochs and 900 non-target epochs. Channels with higher discrimination are usually over the parietal and parietal/occipital regions (typically, PO7 and PO8 provide the higher levels of discrimination). For C-FMS filtered data, the r-square was

computed from projections obtained in (20). Projection 1 is the output of FC beamformer, $\mathbf{y_1}$, and projection 2 is the output of Max-SNR beamformer, $\mathbf{z_1}$. The remaining projections are obtained from $\mathbf{Z}^{(2:N-1)}$ (18). As expected, the first C-FMS projection shows the higher r-square discrimination, increasing the pre-filter maximum of approximately 0.3 to a 0.6 post-filter maximum. Although lower, the second projection of C-FMS also shows some degree of discrimination. The other projections show no discrimination. This result confirms that FC and Max-SNR outputs retain the most discriminative information. Figure 6 shows the mean, $\mu(t)$, and mean $\pm$ standard deviations, $\mu(t) \pm \sigma(t)$, of target and non-target epochs measured at each instant t at channel Cz before spatial filtering (top), and $\mu(t)$ and $\mu(t) \pm \sigma(t)$ of first C-FMS projection (bottom). The increased margin of separation between the patterns of the two classes after C-FMS filtering is remarkable. Figure 7 shows also the effect of spatial filtering in the frequency domain. The plot represents the average of the FFTs spectra of the first spatial projection. Comparing with Fig. 2(d), it can be seen that the 5 Hz interference is almost eliminated from target epochs.

4.2. Spatial Filtering Robustness

The ERP exhibits an inter-trial variability regarding latency, amplitude and morphology. However, there is a spatial correlation between channels (scalp distribution) that is invariant across trials in normal conditions. The estimation of spatial filters takes advantage of this spatial correlation which gives the spatial filter the property of robustness to inter-trial variability. To test the robustness of spatial filtering, we compared the FC beamformer estimated from two independent data sets obtained from the same subjects. Figure 8 shows the weights of the two filters obtained from one subject of the able-bodied group, one subject of the CP group and one subject of the ALS group. The weights of the spatial filters obtained from the two data sets are very similar. These and similar results give good indications that the spatial filters provide a good generalization without training overfitting.

4.3. Offline Classification Results

For each participant, the classification models were obtained from one training data set collected during the calibration session. A second data set, with the same amount of data, was collected for testing, such that all offline results presented in this section were obtained from unseen data.

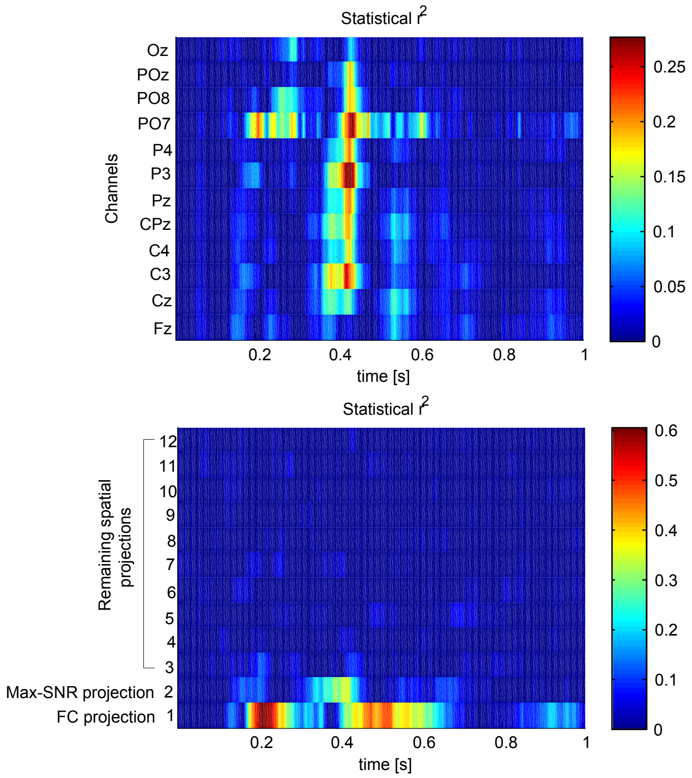

Figure 5: Results obtained from representative data of one session: 180 target epochs and 900 non-target epochs using a 5-epoch average. Color map representing the r-square statistical measure of the discrimination between target and non-target classes. Top: r-square of channels Fz, Cz, C3, C4, CPz, Pz, P3, P4, PO7, PO8, POz and Oz before spatial filtering $(\mathbf{X}_+, \mathbf{X}_-)$. Bottom: r-square of projections of C-FMS beamformer according to (20), where projection 1 is the output of FC beamformer, $\mathbf{y_1}$, and projection 2 is the output of Max-SNR beamformer, $\mathbf{z_1}$. The remaining projections are $\mathbf{Z}^{(2:N-1)}$ according to (18).

The classification performance is assessed using the NB classifier (21), (22), (23). Since the target and non-target classes are highly unbalanced, the measure of error was $\frac{FNR+FPR}{2}$, where FNR and FPR denote respectively false negative rate and false positive rate. Opting for testing on an equal number of target and non-target epochs would be misleading because the classifier assumes different target and non-target probabilities. Two approaches were followed. In the first, the spatial filtering was applied to the average of K-epoch and then the *a posteriori* probability obtained according

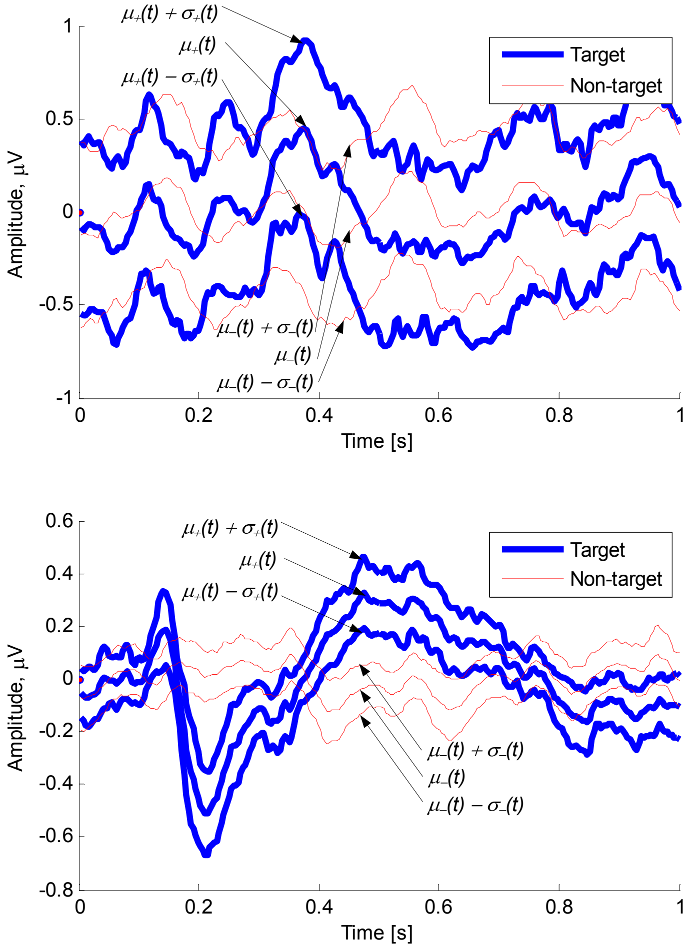

Figure 6: Results obtained from the same data shown in Fig. 5. Top: mean, $\mu(t)$, and mean $\pm$ standard deviation, $\mu(t) \pm \sigma(t)$, of 180 target epochs and 900 non-target epochs measured at channel Cz using a 5-epoch average; Bottom: $\mu(t)$ and $\mu(t) \pm \sigma(t)$ of the first C-FMS projection, $\mathbf{y_1}$, of the 5-epoch average of 180 target epochs and 900 non-target epochs.

to

$$P(C_i|\mathbf{y}) \equiv P(C_i|\frac{1}{K}\sum_{k=1}^{K}\mathbf{y_k}) \qquad , i \in \{+,-\}. \tag{25}$$

In the second approach, the spatial filtering was applied to single epochs and

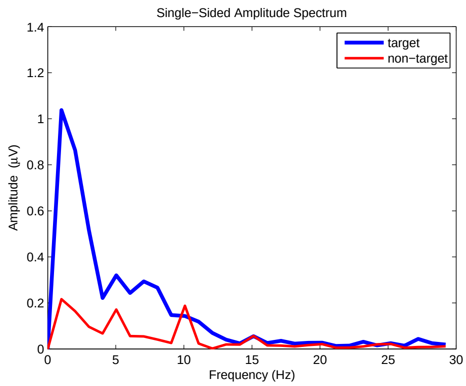

Figure 7: Average of the FFT spectra of the first projection obtained from C-FMS filtered epochs (180 FFTs of target epochs and 900 FFTs of non-target epochs).

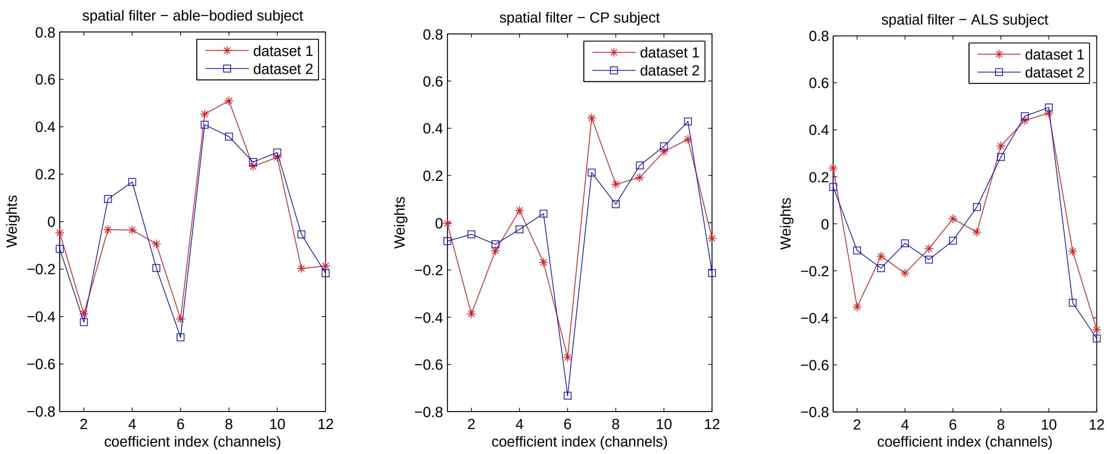

Figure 8: Comparison of FC beamformer estimated from two independent data sets. Results obtained from one subject of the able-bodied group (left), one subject of the CP group (middle), and one subject of the ALS group (right).

then the K-posterior probabilities were combined according to

$$P(C_i|\mathbf{y}) \equiv \prod_{k=1}^{K} P(C_i|\mathbf{y_k}) \qquad , i \in \{+,-\} \tag{26}$$

where $P(C_i|\mathbf{y_k})$ is the *a posteriori* probability for the epoch k and K is the number of epochs (repetitions). Class detection was done in both cases using $P(C_i|\mathbf{y})$ in (23).

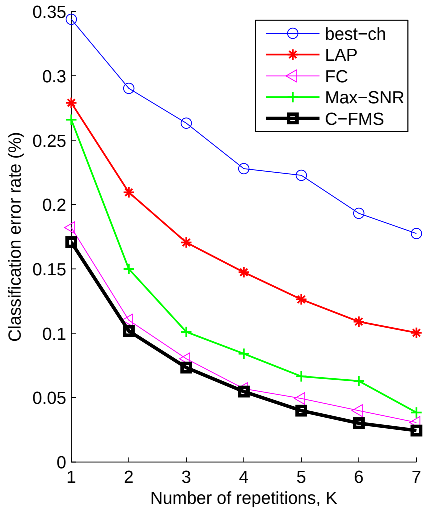

Figure 9: Classification results using the K-epoch average approach for $K \in \{1, \cdots, 7\}$. The results are the averaged values obtained from 23 subjects.

Figure 9 shows the classification error rate following the K-epoch average approach. The error rate was obtained averaging the results of all 23 subjects, i.e., using $23 \times 180 = 4140$ target epochs and $23 \times 900 = 20700$ non-target epochs. The plot shows results of the the 3 proposed spatial filters, and for sake of comparison, the results of the Laplacian derivations, as well as the results concerning the channel presenting the highest discrimination. Figure 9 shows that the classification accuracy increases sharply, for all methods, for $K \leq 3$. For a single epoch ($K = 1$), the spatial filter C-FMS, when compared respectively with the best channel, Laplace derivations, Max-SNR and FC, presents a reduction in the error rate of about 17.3% (t(22)=16.95 $p \leq 0.001$), 10.8% (t(22)=12.17 $p \leq 0.001$), 9.5% (t(22)=5.10 $p \leq 0.001$) and 1.1% (t(22)=3.65 $p = 0.0014$). For $K \geq 2$ these differences remain constant or slightly decrease for best channel, Laplace derivations and FC. For Max-SNR the difference decreases to approximately 5%. This result shows that the Max-SNR filter benefits from higher SNR levels. For best channel and Laplace derivations, their differences to C-FMS are always statistically significant ($p \leq 0.001$). For Max-SNR and FC, their differences to C-FMS for a given K provide the following statistical values: $K = 2$, $p \leq 0.001$ for Max-SNR and $p \leq 0.01$ for FC; $K = 3$, $p \leq 0.005$ for Max-SNR and $p = 0.056$ for

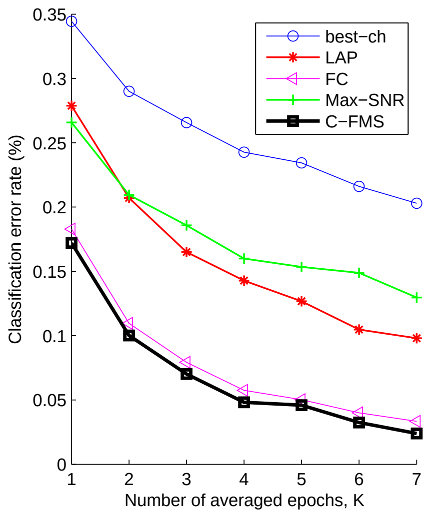

Figure 10: Classification results using the K-probability approach for $K \in \{1, \cdots, 7\}$. The results are the averaged values obtained from 23 subjects.

FC; $K = 4$, $p \leq 0.05$ for Max-SNR and $p = 0.52$ for FC; $K = 5$, $p \leq 0.05$ for Max-SNR and $p = 0.067$ for FC; $K = 6$, $p = 0.084$ for Max-SNR and $p \leq 0.02$ for FC; $K = 7$, $p \leq 0.005$ for Max-SNR and $p = 0.13$ for FC. The difference between C-FMS and FC fails the significance test for some values of K. Comparing Fig. 4 and Fig. 9 a direct relationship between SNR and classification results becomes apparent, i.e., methods with higher SNR provide a better classification. The exception goes to the Laplacian derivations, which shows a better classification than best channel and notwithstanding similar SNRs.

In the K-probability approach, the NB classifier is applied to single epochs and the probabilities are combined using (26). Figure 10 presents the classification results. The statistical t-test was again applied to evaluate the significance of the results. For a single epoch, the results are coincident with the K-epoch approach, since for $K = 1$, (26) is equal to (25). For $K = 2 \cdots 7$ the reduction of classification error rates between C-FMS, and best channel, Laplace derivations and FC, is very similar to the K-epoch average approach. The differences are statistically significant with $p \leq 0.001$ for best channel and Laplace derivations, and $p \leq 0.005$ for FC. The Max-SNR results are poorer than for the K-epoch average. The difference between C-FMS and

Max-SNR is about 10% ($p \leq 0.001$). As referred above, these results show that Max-SNR works better with data with higher SNR provided by the K-epoch average approach. The C-FMS filter is not affected because the feature selection algorithm selects mainly features from the FC filter.

4.4. Online Results

In online operation, the binary classifier is applied to each one of the 12 events. Each event is classified as target or non-target with an associated *a posteriori* probability using (25) or (26). The selected method for our online experiments was the K-epoch approach (25). The final decoded symbol (detected row number, #row, and detected column number, #column) is obtained from the combination of the *a posteriori* probabilities according to

$$\begin{aligned}
&\text{if the number of events detected as target is} \geq 1, \quad \text{then} \\
&\#_{row} = \underset{j\in\{1,\cdots,6\}}{\arg\max}\, P_{+}^{j} \;\wedge\; \#_{col} = \underset{l\in\{1,\cdots,6\}}{\arg\max}\, P_{+}^{l} \\
&\text{else, if all events are detected as non-target,} \quad \text{then} \\
&\#_{row} = \underset{j\in\{1,\cdots,6\}}{\arg\min}\, P_{-}^{j} \;\wedge\; \#_{col} = \underset{l\in\{1,\cdots,6\}}{\arg\min}\, P_{-}^{l}
\end{aligned} \tag{27}$$

where $P_{\{+,-\}}^{\{j,l\}}$ are the *a posteriori* probabilities associated the events of rows (index j) and columns (index l). By words, if more than one event is detected as target, the method chooses the event most likely to be a target. If all the events are detected as non-target, then the method chooses the event less likely to be a non-target.

Each online session occurred after the respective calibration session. The classification models were tested offline and it was selected the least number of repetitions, K, for which an error rate up to 5-10% was found. The number of repetitions was then adjusted, when necessary, according to the online performance of the subject. The C-FMS was the selected spatial filter since it consistently provided better results during the pilot experiments and throughout the sessions in this study as confirmed by the offline analysis in the last section.

Under the same conditions that occurred during the calibration sessions, the subjects were asked to write a sentence. Subjects S1 to S12 (see Table 2) wrote the sentence 'THE-QUICK-BROWN-FOX-JUMPS-OVER-LAZY-DOG' (39 characters), subjects S13 to S19 wrote the sentence 'THE-QUICK-BROWN-FOX' (19 characters) and subjects S20 to S24 wrote the Portuguese sentence 'ESTOU-A-ESCREVER' (16 characters) which means in English ('I am writing'). Participants S13 to S24 wrote a shorter sentence since they underwent an additional paradigm during the same sessions (for a study beyond the scope of this paper). The sentences were written at once without interruptions. In case of error, subjects could opt to correct the character using the 'del' symbol.

To assess the online classification and for comparison with state of the art results it was computed the number of decoded symbols per minute (SPM), and the bandwidth, B, according to (Wolpaw et al., 2000)

$$B = M\left[\log_2(N_s) + P_{ac}\log_2(P_{ac}) + (1-P_{ac})\log_2\frac{(1-P_{ac})}{(N_s-1)}\right] \tag{28}$$

where N_s is the number of possible selections (36 symbols), P_{ac} is the accuracy, and M is the number of possible decisions per minute. The parameter M takes into consideration the number of event repetitions and ISI time. Table 2 summarizes the online results, showing the number of SPM and the associated number of repetitions (NRep), and respective accuracy and bandwidth measured in bit/min (bpm). The online accuracy, P_{ac}, was measured according to

$$P_{ac} = 1 - \frac{N_e}{N_c + N_{ce}} \tag{29}$$

where N_e is the number of misspelled characters/symbols, N_c is the number of characters of the sentence and N_{ce} is the number of corrected errors with 'del'. The average of the results are presented for each group of subjects. Group 1 (S1-S12) spelled on average 4.3 SPM with a success rate of 91.01% corresponding to a bandwidth of 18.78 bpm. The best result was achieved by subject S11 who wrote the sentence with 100% accuracy requiring only 3 repetitions. Group 2 (S13-S19) spelled on average 4.89 SPM with a success rate of 90.32% (bandwidth of 21.31 bpm). These results are better than for group 1, which is understandable because the spelled sentence is shorter and therefore less susceptible to fatigue. The best result was achieved by subject S18 who wrote the sentence with 95% accuracy requiring only 2 repetitions. From the group of participants with CP, subject S21 was unable to perform the online session because the algorithms did not detect target events with an accuracy above 80% even for $K \geq 7$, which was insufficient for online operation. The averaged results were obtained only from S20 and S22. This group spelled on average 3.13 SPM with a success rate of 96.68% (bandwidth of 15.12 bpm). The group of ALS participants spelled on average 3.75 SPM with a success rate of 96.87% (bandwidth of 18.15 bpm). The SPM was computed omitting the ITI of 2.5 seconds. Taking into account the ITI time, the SPM averages were respectively 3.63, 3.96, 2.76 and 3.24 for group 1, 2, 3 and 4. Comparing the results of able-bodied and disabled participants, and taking the bandwidth as the main parameter, we see that on average the results are only slightly lower for disabled participants. It is worth noting that almost all SPM values were obtained for classification accuracies above 85%. Many of the participants wrote the sentences with a fewer number of repetitions (some of them with a single repetition) but with lower accuracies, so we chose not to show these results. Comparing the online and offline results (see Table 3), we can observe that the achieved results for similar SPM and accuracy are just slightly lower for online than for offline. These results corroborate that the online experiments validate the offine results.

4.5. Benchmarking dataset

For performance comparison purposes, the C-SMF filter was tested on the benchmark data sets available for the BCI-Competition 2003 (BCI-Competition, 2003). Simulating the conditions of the competition, we trained the spatial filter, feature selection and classifier from labeled data sets (sessions 10 and 11), which were then tested on unlabeled data sets (session 12), for a different number of repetitions. The inferred words and error rates are shown at Table 4. The achieved results are very competitive with ones presented in (BCI-Competition, 2003).

5. Discussion and Conclusion

This paper has shown that statistical spatial filtering is an effective approach to increase the SNR of ERP components. As a direct consequence, the P300 component is enhanced and classified with a higher accuracy. There are two different trends in the BCI literature for EEG signal classification: spatial filtering preprocessing followed by classification, and spatiotemporal classification (where feature vectors are the concatenation of spatiotemporal features). As was seen in section 4.2, spatial filtering results give indications of good generalization properties, which provides an important argument to use the spatial filtering approach. From a neurophysiologic perspective, the spatial filtering provides enhanced versions of the input signals. From one hand, this contributes to a better signal interpretation by neurophysiologists

Table 2: Online results.

Subject	SPM (NRep)	P_{ac} (%)	Bandwidth (bpm)
S1	4.68 (4)	95.12	21.74
S2	3.75 (5)	95.12	17.39
S3	3.75 (5)	86.67	14.69
S4	6.25 (3)	95.12	28.99
S5	3.75 (5)	95.12	17.39
S6	3.75 (5)	86.67	14.69
S7	2.67 (7)	90.70	11.37
S8	3.75 (5)	79.59	12.72
S9	4.68 (4)	90.70	19.90
S10	3.75 (5)	90.70	15.92
S11	6.25 (3)	100.0	**32.31**
S12	4.68 (4)	86.67	18.37
Average 1	4.30 (4.6)	91.01	18.79
S13	2.67 (7)	84.21	9.99
S14	3.75 (5)	82.60	13.54
S15	3.75 (5)	100.0	19.38
S16	4.68 (4)	90.47	19.81
S17	3.75 (5)	85.00	14.21
S18	9.38 (2)	95.00	**43.38**
S19	6.25 (3)	95.00	28.91
Average 2	4.89 (4.4)	90.32	21.31
S20	3.13 (6)	100.0	**16.15**
S21	-	-	-
S22	3.13 (6)	93.37	14.10
Average 3	3.13 (6)	96.68	15.12
S23	3.75 (5)	100.0	**19.38**
S24	3.75 (5)	93.75	16.92
Average 4	3.75 (5)	96.87	18.15
Overall Average	4.33 (4.7)	91.80	19.18

Table 3: SPM and bandwidth using the offline classification accuracy obtained in Fig. 9 with C-FMS.

	Number of repetitions (K)						
	1	2	3	4	5	6	7
P_{ac}(%)	82.92	89.82	92.66	94.52	96.01	96.99	97.56
SPM	18.75	9.37	6.25	4.68	3.75	3.12	2.67
bpm	68.14	39.12	27.59	21.48	17.71	15.06	13.07

or psychologists, because it preserves and accentuates the biomarkers, and on the other hand it can reduce the duration time of clinical tests.

Table 4: Inferred words and associated error rates for different number of repetitions, using data sets from BCI - Competition 2003.

NRep	Inferred words	Error
1	FCOD MMON BBM JIC CAAC TTNB ZTBUT XXX1	58.0 %
2	FCOD GMOT BAM JIE CALC TCNA ZMAOT X0Z7	41.9 %
3	FOOD MOOT HAM JIE CAKC TCNA ZSAOT X457	25.8 %
4	FOOD MOOT HAM PIE CAKE TUNA ZYGOT 4567	0.0 %

Following the K-epoch average approach, the three proposed spatial filters showed higher classification accuracy than those obtained with Laplacian derivations and best channel. Following the K-probability approach, the Max-SNR beamformer had a lower performance than Laplace derivations, however FC and C-FMS remained with higher accuracies. The classification accuracy of C-FMS filter was statistically higher than all other methods using both approaches.

The gold standards to evaluate a BCI performance should be the online accuracy and online bandwidth. Only these parameters can attest the effective application of BCI in real world scenarios. Additionally, the requirement of a reduced time (ideally a zero time) for calibration is also an important issue for effective use of BCI. We demonstrate in this paper that the proposed methodology provides efficient accuracy and bandwidth for able-bodied subjects and subjects with CP and ALS. Considering only the group of able-bodied participants, the achieved online results were on average 4.3 SPM with a success rate of 91.01% and a respective bandwidth of 18.78 bpm for group 1, and 4.89 SPM, 90.32%, 18.79 bpm for group 2. These results are higher than those found in (Farwell and Donchin, 1988; Serby et al., 2005; Thulasidas et al., 2006; Krusienski et al., 2008) and similar to the ones presented in (Lenhardt et al., 2008), which presents an effective SPM (including ITI) of 3.91 with 83.33% mean accuracy in comparison to our result of 3.63 SPM (including ITI) with a 91.01% accuracy for group 1, and 3.96 SPM (including ITI) with 90.32% accuracy for group 2. The results were obtained for 12 subjects with a sentence of 22 characters, while in our case the sentences had lengths of 39 and 19 characters, tested by 19 participants. Considering the group of subjects suffering from CP and ALS, only subject S21 was unable to perform the online task. Apparently, the high amplitude of nonvoluntary movements affected his attention to relevant targets, but there may be other neurophysiologic causes. The other ALS and

CP participants achieved, on average, results just slightly lower than those achieved by able-bodied. The results are good in comparison with other studies reported in the state of the art. However, the results can not be directly comparable because there are many different parameters to take into account, namely, different levels of functionality, different pathologies and stage of the disease, different number of sessions (extension of the study), and different visual paradigms. For the purpose of comparison of P300 BCI studies on people with motor disabilities, the following recent studies are suggested. In (Nijboer et al., 2008), 10 subjects with advanced ALS tested a 6×6 and a 7×7 matrix speller paradigm. Two 8×9 speller paradigms were compared by 3 advanced ALS participants in (Townsend et al., 2010). Donchin et al. (2000) describes a study with 4 paraplegic participants who tested a 6×6 matrix speller paradigm. Five subjects with different motor disabilities (ALS, locked-in, spinal cord injury, multiple sclerosis and Guillain Barre syndrome) tested a 4 choice paradigm in (Piccione et al., 2006). The study in (Sellers and Donchin, 2006) reports 4 choice paradigm tested by 3 ALS subjects but all with communication ability. In (Hoffmann et al., 2008a) 5 subjects with different motor disabilities (CP, multiple sclerosis, late-stage ALS, spinal cord injury and post-anoxic encephalopathy) tested a 6 choice visual paradigm. It is worth to note that this last study is the only reported work on P300 based BCIs that includes a CP subject. The achieved results in our study indicate the effective possibility of people with severe CP to be able to use a BCI as a communication channel. Taking into consideration that the participants were non-experienced users, it is expected that they can still improve their performances. The use of our BCI as an alternative to other standard interfaces still requires a higher bandwidth. For instance, subject S20 uses in his daily life a scanning interface controlled by an head switch to write. The number of selected symbols per minute is on average 6.5, i.e., twice of what he achieved with our BCI system. Furthermore, the strong involuntary movements of the head and the body of some subjects can be a limitative factor for the use of a P300-based BCI. The good results obtained with ALS participants are encouraging. However, they only had their spoken communication affected, still retaining other alternative means of communication.

For a more robust evaluation, the next step is to extend the study to a larger group of CP patients and include ALS patients in more advanced stages.

Acknowledgment

The authors would like to thank to all participants who volunteered to experiments and also to APCC and HUC staff. This work was supported in part by Fundação para a Ciência e Tecnologia (FCT), under Grant RIPD/ADA/109661/2009.

References

BCI-Competition . BCI competition 2003 - data set IIb. http://www.bbci.de/competition/ii/; 2003.

Blanchard G, Blankertz B. BCI competition 2003-data set IIa: spatial patterns of self-controlled brain rhythm modulations. IEEE Trans Biomed Eng 2004;51(6):1062–6.

Cedarbaum JM, Stambler N, Malta E, Fuller C, Hilt D, Thurmond B, Nakanishi A. The ALSFRS-R: a revised ALS functional rating scale that incorporates assessments of respiratory function. J the Neurological Sciences 1999;169(1-2):13 – 21.

de Cheveigne A, Simon JZ. Denoising based on spatial filtering. J Neurosci Methods 2008;171(2):331–9.

Donchin E, Spencer K, R. W. The mental prosthesis: Assessing the speed of a P300-based brain-computer interface. IEEE Trans Rehabil Eng 2000;8(2):174–9.

Dornhege G, Blankertz B, Krauledat M, Losch F, Curio G, Müller KR. Combined optimization of spatial and temporal filters for improving brain-computer interfacing. IEEE Trans Biomed Eng 2006;53(11):2274–81.

Duda R, Hart P, Stork D. Pattern Classification. Wiley London UK, 2001.

Farwell L, Donchin E. Talking off the top of your head: toward a mental prosthesis utilizing event related brain potentials. Electr and Clin Neuroph 1988;70(6):510–23.

Fukunaga K. Introduction to Statistical Pattern Recognition, Second Edition. Morgan Kaufmann - Academic Press, 1990.

Fukunaga K, Koontz WG. Application of the Karhunen-Loeve Expansion to Feature Selection and Ordering. IEEE Trans Computers 1970;C-19(4):311–8.

Grosse-Wentrup M, Liefhold C, Gramann K, Buss M. Beamforming in noninvasive brain-computer interfaces. IEEE Trans Biomed Eng 2009;56(4):1209–19.

Hall MA. Correlation-based feature selection for discrete and numeric machine learning. In: Proc. 17th Int. Conf. Machine Learning. 2000. p. 359–66.

Hoffmann U, Vesin J, Ebrahimi T. Spatial filters for the classification of event-related potentials. In: Eur. Symp. Artificial Neural Networks. 2006. p. 47–52.

Hoffmann U, Vesin JM, Ebrahimi T, Diserens K. An efficient P300-based brain-computer interface for disabled subjects. J Neuroscience Methods 2008a;167(1):115–25.

Hoffmann U, Yazdani A, Vesin JM, Ebrahimi T. Bayesian Feature Selection Applied In a P300 Brain- Computer Interface. In: 16th Eur. Signal Processing Conference. 2008b. .

Ivannikov A, Kalyakin I, Hamalainen J, Leppanen PH, Ristaniem T, Lyytinen H, Karkkainen T. ERP denoising in multichannel EEG data using contrasts between signal and noise subspaces. J Neurosci Methods 2009;180(2):340–51.

Jung TP, Makeig S, Westerfield M, Townsend J, Courchesne E, Sejnowski TJ. Removal of eye activity artifacts from visual event-related potentials in normal and clinical subjects. Clin Neurophysiol 2000;111(10):1745–58.

Kaper M, Meinicke P, Grossekathoefer U, Lingner T, Ritter H. BCI competition 2003-data set IIb: support vector machines for the P300 speller paradigm. IEEE Trans Biomed Eng 2004;51(6):1073–6.

Krusienski D, Sellers E, Cabestaing F, Bayoudh S, McFarland D, Vaughan T, Wolpaw J. A comparison of classification techniques for the P300 speller. J neural Eng 2006;(3):299–305.

Krusienski D, Sellers S, D. McFarland T. Vaughan JW. Toward enhanced P300 speller performance. J Neurosci Methods 2008;167(1):15–21.

Krusienski DJ, Sellers W, Vaughan TM. Common spatio-temporal patterns for the P300 speller. In: 3rd IEEE EMBS Intern. Conf. Neural Eng. 2007. p. 421–4.

Lemm S, Blankertz B, Curio G, Müller KR. Spatio-spectral filters for improving the classification of single trial EEG. IEEE Trans Biomed Eng 2005;52(9):1541–8.

Lemm S, Curio G, Hlushchuk Y, Müller KR. Enhancing the signal-to-noise ratio of ICA-based extracted ERPs. IEEE Trans Biomed Eng 2006;53(4):601–7.

Lenhardt A, Kaper M, Ritter H. An adaptive P300-based online braincomputer interface. IEEE Trans Neural Syst and Rehabil Eng 2008;16(2):121–30.

Li Y, Gao X, Liu H, Gao S. Classification of single-trial electroencephalogram during finger movement. IEEE Trans Biomed Eng 2004;51(6):1019–25.

Makeig S, Westerfield M, ping Jung T, Covington J, Townsend J, Sejnowski TJ, Courchesne E. Functionally independent components of the late positive event-related potential during visual spatial attention. J Neurosci 1999;19(7):2665–80.

McFarland DJ, McCane L, David SV, Wolpaw JR. Spatial filter selection for EEG-based communication. Electroenceph Clin Neurophysiol 1997;103:386–94.

Mell D, Bach M, Heinrich SP. Fast stimulus sequences improve the efficiency of event-related potential p300 recordings. J Neurosci Methods 2008;174(2):259 –64.

Müller KR, Vigario R, Meinecke F, Ziehe A. Blind source separation techniques for decomposing event related brain signals. Int J Bifurcation and Chaos 2004;14(2):773–91.

Müller-Gerking J, Pfurtscheller G, Flyvbjerg H. Designing optimal spatial filters for single-trial EEG classification in a movement task. Clin Neurophysiol 1999;110(5):787–98.

Naeem M, Brunner C, Leeb R, Graimann B, Pfurtscheller G. Seperability of four-class motor imagery data using independent components analysis. J Neural Eng 2006;3(3):208–16.

Nijboer F, Sellers E, Mellinger J, Jordan M, Matuz T, Furdea A, Halder S, Mochty U, Krusienski D, Vaughan T, Wolpaw J, Birbaumer N, Kbler A. A P300-based brain-computer interface for people with amyotrophic lateral sclerosis. Clin Neurophysiol 2008;119(8):1909 –16.

Piccione F, Giorgi F, Tonin P, Priftis K, Giove S, Silvoni S, Palmas G, Beverina F. P300-based brain computer interface: Reliability and performance in healthy and paralysed participants. Clin Neurophysiol 2006;117(3):531–7.

Pires G, Nunes U, Castelo-Branco M. P300 spatial filtering and coherence-based channel selection. In: 4th Int. IEEE EMBS Conf. Neural Eng., NER09. 2009. p. 311–4.

Rakotomamonjy A, Guigue V. BCI competition III: Dataset II- ensemble of svms for BCI P300 speller. IEEE Trans Biomed Eng 2008;55(3):1147–54.

Ramoser H, Müller-Gerking J, Pfurtscheller G. Optimal spatial filtering of single trial EEG during imagined hand movement. IEEE Trans Rehabil Eng 2000;8(4):441–6.

Rivet B, Souloumiac A, Attina V, Gibert G. xDAWN algorithm to enhance evoked potentials: Application to Brain-Computer Interface. IEEE Trans Biomed Eng 2009;56(8):2035 –43.

Sekihara K, Nagarajan S, Poeppel D, Marantz A, Miyashita Y. Reconstructing spatio-temporal activities of neural sources using an meg vector beamformer technique. IEEE Trans Biomed Eng 2001;48(7):760 –71.

Sellers EW, Donchin E. A P300-based brain-computer interface: Initial tests by als patients. Clin Neurophysiol 2006;117(3):538 –48.

Serby H, Yom-Tov E, Inbar G. An improved P300-based brain-computer interface. IEEE Trans Neural Syst and Rehabil Eng 2005;13:89–98.

Soong A, Koles Z. Principal-component localization of the sources of the background EEG. IEEE Trans Biomed Eng 1995;42(1):59–67.

Srinivasan R, Nunez P, Silberstein R. Spatial filtering and neocortical dynamics: estimates of EEG coherence. IEEE Trans Biomed Eng 1998;45(7):814–26.

Thulasidas M, Guan C, Wu J. Robust classification of EEG signal for brain-computer interface. IEEE Trans Neural Syst and Rehabil Eng 2006;14(1):24–9.

Tomioka R, Aihara K, Müller KR. Logistic regression for single trial EEG classification. In: Schölkopf B, Platt J, Hoffman T, editors. Advances in Neural Information Processing Syst. 19. MIT Press; 2007. p. 1377–84.

Townsend G, LaPallo B, Boulay C, Krusienski D, Frye G, Hauser C, Schwartz N, Vaughan T, Wolpaw J, Sellers E. A novel P300-based brain-computer interface stimulus presentation paradigm: Moving beyond rows and columns. Clin Neurophysiol 2010;121(7):1109 –20.

Trees HV. Optimum Array Processing. Part IV of Detection, Estimation and Modulation Theory, 2002.

Van Veen B, Van Drongelen W, Yuchtman M, Suzuki A. Localization of brain electrical activity via linearly constrained minimum variance spatial filtering. IEEE Trans Biomed Eng 1997;44(9):867 –80.

Van Veen BD, Buckley KM. Beamforming: A versatile approach to spatial filtering. IEEE Signal Processing Magazine 1988;5(2):4–24.

Wolpaw J, Birbaumer N, Heetderks W, McFarland D, Peckham P, Schalk G, Donchin E, Quatrano L, Robinson C, Vaughan T. Brain-computer interface technology: a review of the first international meeting. IEEE Trans Rehabil Eng 2000;8(2):164–73.

Xu N, Gao X, Hong B, Miao X, Gao S, Yang F. BCI competition 2003-data set IIb: enhancing P300 wave detection using ICA-based subspace projections for BCI applications. IEEE Trans Biomed Eng 2004;51(6):1067 –72.